SLAC-PUB-16229

A Massively Parallel Solver for Mechanical Harmonic Analysis of Accelerator Cavities

O. Kononenko

SLAC National Accelerator Laboratory
2575 Sand Hill Road, Menlo Park, CA 94025, USA
E-mail: Oleksiy.Kononenko@slac.stanford.edu

Abstract

ACE3P is a 3D massively parallel simulation suite that developed at SLAC National Accelerator Laboratory that can perform coupled electromagnetic, thermal and mechanical study. Effectively utilizing supercomputer resources, ACE3P has become a key simulation tool for particle accelerator R&D. A new frequency domain solver to perform mechanical harmonic response analysis of accelerator components is developed within the existing parallel framework. This solver is designed to determine the frequency response of the mechanical system to external harmonic excitations for time-efficient accurate analysis of the large-scale problems. Coupled with the ACE3P electromagnetic modules, this capability complements a set of multi-physics tools for a comprehensive study of microphonics in superconducting accelerating cavities in order to understand the RF response and feedback requirements for the operational reliability of a particle accelerator.

Keywords: Particle accelerators, parallel computing, harmonic analysis, structural mechanics

1. Introduction

Many mechanical systems are subject to external loading that varies harmonically with time [1]. As a consequence, the loading causes a sustained cyclic response in a structure often referred to as a harmonic response. A corresponding analysis must be performed to study this behavior of mechanical structures and verify whether or not the designs will successfully overcome resonance, fatigue, and other harmful effects of forced vibrations.

In superconducting accelerator modules the external loading and subsequent mechanical vibrations are often translated into undesired electrical signals, so-called microphonics, affecting operational reliability of the particle accelerator. In particular, a superconducting cavity [2-3] with a high quality factor and a narrow frequency bandwidth has a high sensitivity to microphonics coming from the oscillations of the environment or the radiation pressure [4].

Accurate design of the accelerating structure can help reduce the microphonics effect to a tolerable level and, hence, gain in efficiency saving the driving power and machine operation costs. A necessary step to perform this study is an accurate calculation of the accelerating structure's behavior as a response to the external harmonic loading.

The finite-element method [5] is used by most harmonic response solvers in structural mechanics and is applicable to study arbitrary complex geometries providing required accuracy. The development of the related commercial software has been mainly targeted on desktop computers although some parallel implementations are available as well. However, for large-

This material is based upon work supported by the U.S. Department of Energy, Office of Science, Office of Basic Energy Sciences, under Contract No. DE-AC02-76SF00515 and ASCR.

scale problems it is advantageous and required to use parallel computing on supercomputer resources for large memory usage and computational time speedup.

For the past decades, the ACE3P simulation suite [6] has been developed at SLAC National Accelerator Laboratory for large-scale accelerator applications using high performance computing. It has been used extensively in the design and optimization studies for many accelerator projects [7-9] becoming a key simulation tool for particle accelerator R&D. The developed harmonic response solver presented in this paper uses the existing software infrastructure of ACE3P including mesh domain decomposition, matrix assembly scheme and implementations of linear solvers and preconditioners.

2. Mathematical Model

2.1 Problem Statement

The governing equations of the linear elasticity are the equation of motion (second Newton's law), the strain-displacement equation and the Hook's law [10]:

$$\nabla \bullet \sigma + F = \rho \ddot{u} \tag{1}$$

$$\varepsilon = \frac{1}{2}\left(\nabla u + \nabla u^T\right) \tag{2}$$

$$\sigma = C\varepsilon \tag{3}$$

where σ and ε are the stress and strain tensors, u is the displacement vector, F is the vector of the external forces, C — the stiffness tensor and ρ is the material density, respectively. These equations hold true in a 3D domain Ω under the linearization assumptions: infinitesimal strains and linear relationships between the components of the stress and strain.

A well-posed problem must also include additional constrains on the domain boundary $\partial\Omega$ [10]. In this paper we consider Dirichlet, i.e. prescribed displacement (4), and Neumann, i.e. prescribed normal loading (5), boundary conditions:

$$u = u_0 \tag{4}$$

$$\sigma \cdot n = t_0 \tag{5}$$

where u_0 is the vector of prescribed displacements, n — the outer normal and t_0 is the traction vector, respectively. Defining a boundary $\partial\Omega$ as Γ, we assume that $\Gamma = \Gamma_D \cup \Gamma_N$, where (4) holds true on Γ_D and (5) on Γ_N, see Fig. 1.

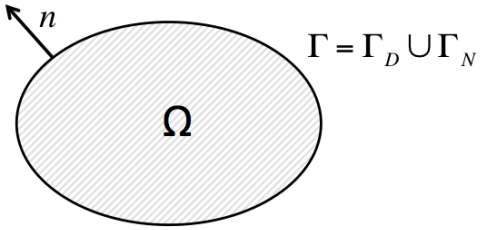

Figure 1. Domain Ω for the problem (1-3) and a boundary Γ where either Dirichlet or Neumann boundary conditions hold true.

We assume that Ω consists of an isotropic material, so that the Hook's law (3) can be explicitly written as:

$$\begin{bmatrix}\sigma_{11}\\ \sigma_{22}\\ \sigma_{33}\\ \sigma_{12}\\ \sigma_{13}\\ \sigma_{23}\end{bmatrix} = \begin{bmatrix}2\mu+\lambda & \lambda & \lambda & 0 & 0 & 0\\ \lambda & 2\mu+\lambda & \lambda & 0 & 0 & 0\\ \lambda & \lambda & 2\mu+\lambda & 0 & 0 & 0\\ 0 & 0 & 0 & \mu & 0 & 0\\ 0 & 0 & 0 & 0 & \mu & 0\\ 0 & 0 & 0 & 0 & 0 & \mu\end{bmatrix}\begin{bmatrix}\varepsilon_{11}\\ \varepsilon_{22}\\ \varepsilon_{33}\\ \varepsilon_{12}\\ \varepsilon_{13}\\ \varepsilon_{23}\end{bmatrix} \tag{6}$$

where λ and μ are Lamé coefficients [10].

To formulate a harmonic response problem, we also assume that there are no external 3D forces involved ($F = 0$) and the external excitation, as well as the resulting field of the displacements, stresses and strains depend harmonically on time, i.e. as $e^{i\omega t}$, where $\omega = 2\pi f$ is the angular frequency, f the frequency, and t the time, respectively. Later we will omit the $e^{i\omega t}$ factor, redefining for simplicity u, u_0, σ, ϵ and t_0 as the corresponding amplitudes of displacements, stresses, strains and traction.

Based on these assumptions we rewrite (1) in Ω as

$$\nabla \cdot \sigma = -\omega^2 \rho u \tag{7}$$

Equations (2,3,7) considered along with boundary conditions (4-5) constitute a harmonic response problem for the linear elasticity equations under the given assumptions for the unknown displacement u and stress σ.

2.2 Weak Formulation and Finite-Element Method

To derive the equivalent integral equation we follow the standard finite-element scheme [5], also used for the mechanical eigenmodes model in ACE3P [11]. Multiplying (7) by a test vector function $v: \mathbb{R}^3 \to \mathbb{R}^3$ and integrating it over the domain Ω we obtain

$$\int_\Omega (\nabla \bullet \sigma) \bullet v d\Omega = -\omega^2 \int_\Omega \rho (u \bullet v) d\Omega \tag{8}$$

Employing divergence theorem [12] the left-hand side of (8) can be represented as

$$\int_\Omega (\nabla \bullet \sigma) \bullet v d\Omega = \int_\Gamma v(\sigma \bullet n) d\Gamma - \int_\Omega \sigma \bullet \nabla v d\Omega$$

Plugging this representation into (8) we obtain:

$$\int_\Gamma v(\sigma \bullet n) d\Gamma - \int_\Omega \sigma \bullet \nabla v d\Omega = -\omega^2 \int_\Omega \rho (u \bullet v) d\Omega$$

Taking into account the boundary condition (4), the first integral can be simplified as $\sigma = 2\mu\frac{1}{2}(\nabla u + \nabla u^T) + \lambda(\nabla \bullet u)I\big|_{\Gamma_D} = 0$. Finally, using similar technique as in [11], we derive a weak form of the problem for the unknown displacement *u*:

$$\int_{\Omega}\left(\mu(\nabla u + \nabla u^T) + \lambda(\nabla \bullet u)I\right) \bullet \nabla v d\Omega = \omega^2 \int_{\Omega} \rho(u \bullet v) d\Omega + \int_{\Gamma_N} (v \bullet t_0) d\Gamma_N \quad (9)$$

The weak form (9) is also applicable to inhomogeneous materials, i.e. when the Lamé coefficients λ and μ as well as the material density ρ are space-dependent.

To numerically solve (9) we employ the nodal basis functions $\varphi_i: \mathbb{R} \to \mathbb{R}$ [13] and express the 3D displacement field as

$$u = (u^x, u^y, u^z) = \left(\sum_{j=1}^{N} u_j^x \phi_j, \sum_{j=1}^{N} u_j^y \phi_j, \sum_{j=1}^{N} u_j^z \phi_j\right)$$

where *N* is the number of nodes in the mesh discretization of Ω, u_i, v_i and w_i are the displacement components at the *i*-th node of the mesh.

Plugging the basis expansion into (9) and taking $v = (\varphi_i, 0, 0)$, $v = (0, \varphi_i, 0)$ and $v = (0, 0, \varphi_i)$ we reduce the integral equation to a linear algebraic system for the unknown displacements and fixed angular frequency:

$$(K - \omega^2 M)\, u = B \quad (10)$$

where K and M are the stiffness and mass matrices respectively, B – is the right-hand side vector. The explicit forms of the matrices and vector can be written as

$$K_{ij} = \begin{bmatrix} k_{11} & k_{12} & k_{13} \\ k_{12} & k_{22} & k_{23} \\ k_{13} & k_{23} & k_{33} \end{bmatrix}_{ij} \qquad M_{ij} = \begin{bmatrix} m_{11} & 0 & 0 \\ 0 & m_{11} & 0 \\ 0 & 0 & m_{11} \end{bmatrix}_{ij} \qquad B_{ij} = \begin{bmatrix} b_1 \\ b_2 \\ b_3 \end{bmatrix}_{ij} \quad (11)$$

where $i, j = \overline{1, N}$ and

$$k_{11} = \int_{\Omega} (2\mu + \lambda)\frac{\partial \varphi_i}{\partial x}\frac{\partial \varphi_j}{\partial x} + \mu\frac{\partial \varphi_i}{\partial y}\frac{\partial \varphi_j}{\partial y} + \mu\frac{\partial \varphi_i}{\partial z}\frac{\partial \varphi_j}{\partial z} d\Omega$$

$$k_{12} = \int_{\Omega} \mu\frac{\partial \varphi_i}{\partial y}\frac{\partial \varphi_j}{\partial x} + \lambda\frac{\partial \varphi_i}{\partial x}\frac{\partial \varphi_j}{\partial y} d\Omega$$

$$k_{13} = \int_{\Omega} \mu\frac{\partial \varphi_i}{\partial z}\frac{\partial \varphi_j}{\partial x} + \lambda\frac{\partial \varphi_i}{\partial x}\frac{\partial \varphi_j}{\partial z} d\Omega$$

$$k_{22} = \int_{\Omega} \mu \frac{\partial \varphi_i}{\partial x}\frac{\partial \varphi_j}{\partial x} + (2\mu + \lambda)\frac{\partial \varphi_i}{\partial y}\frac{\partial \varphi_j}{\partial y} + \mu \frac{\partial \varphi_i}{\partial z}\frac{\partial \varphi_j}{\partial z} d\Omega$$

$$k_{23} = \int_{\Omega} \mu \frac{\partial \varphi_i}{\partial z}\frac{\partial \varphi_j}{\partial y} + \lambda \frac{\partial \varphi_i}{\partial y}\frac{\partial \varphi_j}{\partial z} d\Omega$$

$$k_{33} = \int_{\Omega} \mu \frac{\partial \varphi_i}{\partial x}\frac{\partial \varphi_j}{\partial x} + \mu \frac{\partial \varphi_i}{\partial y}\frac{\partial \varphi_j}{\partial y} + (2\mu + \lambda)\frac{\partial \varphi_i}{\partial z}\frac{\partial \varphi_j}{\partial z} d\Omega$$

$$m_{11} = \int_{\Omega} \rho \varphi_i \varphi_j d\Omega$$

$$b_1 = \int_{\Gamma_N} t_0^x \varphi_i d\Gamma_N \quad b_2 = \int_{\Gamma_N} t_0^y \varphi_i d\Gamma_N \quad b_3 = \int_{\Gamma_N} t_0^z \varphi_i d\Gamma_N$$

The boundary conditions (4-5) are imposed in the following way:

- Dirichlet, the magnitude of the harmonic oscillation of the node is fixed in all three directions
- Neumann, the magnitude of the harmonic normal loading is fixed in all three directions
- Mixed, the magnitude of the harmonic oscillations is fixed in some directions and the magnitude of the harmonic normal loading is fixed in other directions, i.e. a component-wise Dirichlet or Neumann boundary condition

It should be mentioned that imposing the boundary conditions, the stiffness and mass matrices become real and symmetric. In addition, *M* is positive definite, and therefore appropriate numerical methods have to be applied to solve the discretized linear system.

3. Software Design and Parallelization

Based on the finite-element mathematical formulation presented in the previous section, a harmonic response solver is implemented involving the existing C++/MPI ACE3P infrastructure [6]. This solver adds a new modelling capability in ACE3P's multi-physics module TEM3P [14], which is designed for integrated electromagnetic, thermal and mechanical analysis of accelerator structures. The simulation workflow of ACE3P is described in details in [11].

The stiffness and mass matrices as well as the right-hand side vector are assembled in parallel according to the patterns (11) and appropriate boundary conditions are imposed. 3D Gaussian quadratures are utilized to calculate the matrix elements. The resulting matrices are sparse and real with the patterns similar to the ones involved in the TEM3P finite-element based static structural solver. Therefore, the direct and iterative solvers already implemented in the module can be readily adapted to solving (10).

4. Convergence and Validation

To validate the proposed method, we consider a problem (1-3) in the hexahedral domain $\Omega = [0, L_x]$ x $[0, L_y]$ x $[0, L_z]$ with the following boundary conditions:

$$u^x = u^y = u^z = 0, \; x \in \{0, \; L_x\} \tag{12}$$
$$u^x = u^y = u^z = 0, \; y \in \{0, \; L_y\} \tag{13}$$
$$u^x = u^y = u^z = 0, \; z = 0 \tag{14}$$
$$\sigma = t_0, \;\; z = L_z \tag{15}$$

These conditions physically correspond to the fixed cuboid with one surface, $z = L_z$, under the harmonic external loading, see Fig. 2 for details.

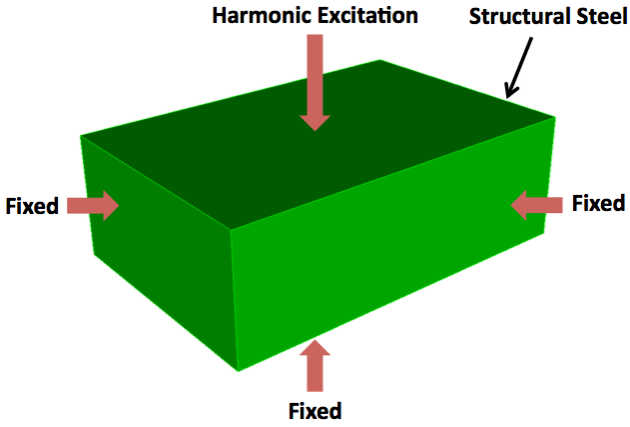

Figure 2. Cuboid domain made of structural steel used for the validation study

Property	**Value**
Density, ρ [kg/m^3]	7850
Poisson Ratio, υ	0.3
Young's Modulus, E [GPa]	200

Table 1. Structural steel properties used in the validation study.

In the convergence and validation study, we consider $L_x = 1$ m, $L_y = 2$ m, $L_z = 3$ m and the cuboid Ω is made of structural steel. See Table 1 for the exact material properties. The loading frequency is considered to be 50 Hz and the amplitude is fixed at 10^{11} Pa.

First, we perform a mesh convergence study of the proposed method. We start from a 2K tetrahedral mesh and increase the size regularly to 84K, roughly doubling the mesh size at each step. We use second order basis functions and calculate the harmonic response of the cuboid. The maximum and minimum displacement amplitudes are shown in the Table 2.

Mesh Size	u^x_{min}	u^x_{max}	u^y_{min}	u^y_{max}	u^z_{min}	u^z_{max}
2000	0	0.37469856	-0.06383108	0.06251243	-0.05923610	0.06016678
7000	0	0.37446038	-0.06543277	0.06522968	-0.06104570	0.06183667
17000	0	0.37463003	-0.06312217	0.06298492	-0.06013235	0.05990996
33000	0	0.37418054	-0.06457493	0.06444406	-0.06090186	0.06077397
59367	0	0.37434851	-0.06420296	0.06405685	-0.06155456	0.06089649
84000	0	0.37434851	-0.06420296	0.06405685	-0.06155456	0.06089649

Table 2. The maximum and minimum displacement amplitudes [m]
for the problem (1-3) with the boundary conditions (12-15).

The relative errors defined as

$$\varepsilon^x = \left|\frac{u^x_N - u^x_{N+1}}{u^x_{N+1}}\right| \quad \varepsilon^y = \left|\frac{u^y_N - u^y_{N+1}}{u^y_{N+1}}\right| \quad \varepsilon^z = \left|\frac{u^z_N - u^z_{N+1}}{u^z_{N+1}}\right|$$

are calculated for the maximum displacement amplitudes in all three direction and are shown in Fig. 3 as a function of the mesh size. It should be noted that the solution is accurate up to eight decimal places when the mesh size is larger than 59K.

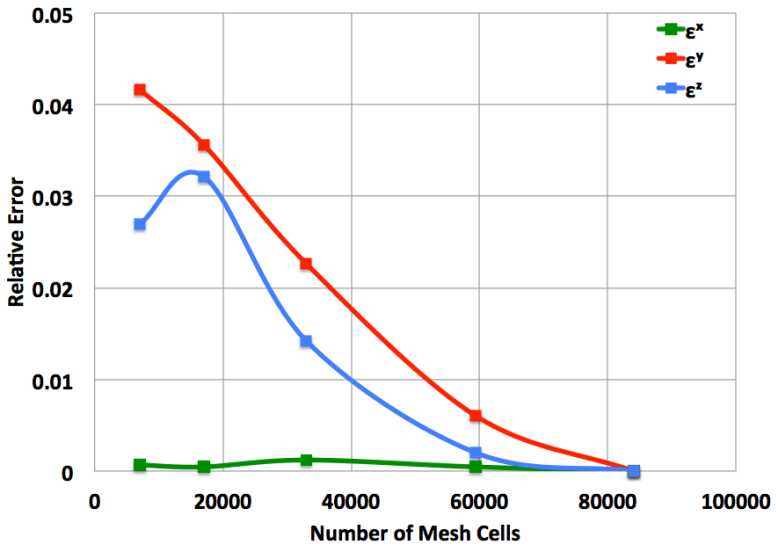

Figure 3. Relative error as a function of the mesh size for the problem (1-3), (12-15).

In Fig. 4 the magnitude of the displacement is benchmarked between ACE3P and ANSYS harmonic response module [15].

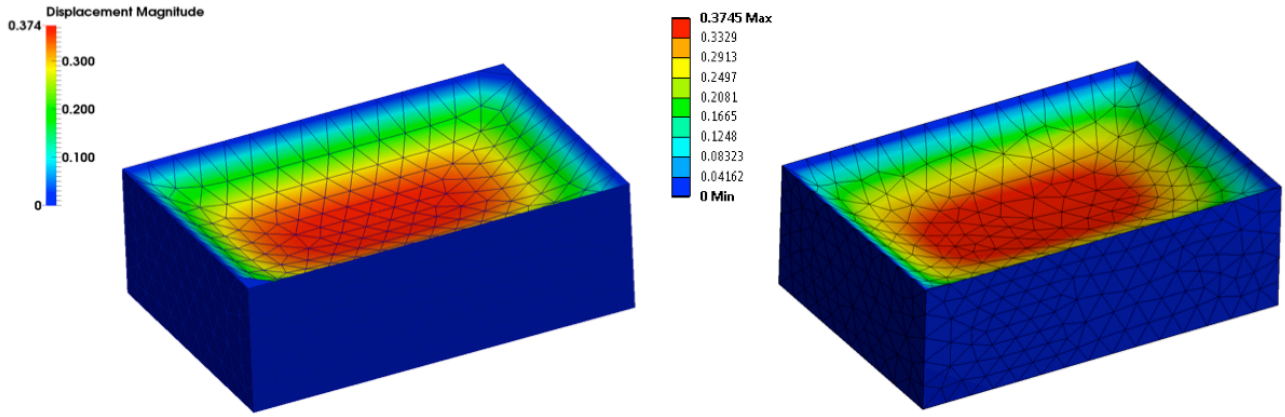

Figure 4. Displacement magnitudes plotted on top of the deformed tetrahedral mesh (shown in black) as calculated using ACE3P (left) and in ANSYS (right).

In this validation example, the harmonic response solver developed in ACE3P has been shown to achieve fast convergence. Moreover, the corresponding displacement fields from ACE3P and ANSYS calculations agree well and have the identical maximum values, as shown in Fig. 4.

We also benchmark the harmonic calculations versus the ACE3P mechanical eigenmode solver [11]. For the harmonic response problem (1-3) with the boundary conditions (12-15), we consider the eigenmodes problem (1-3) and the boundary conditions (12-14, 16):

$$\sigma = 0, \quad z = L_z \tag{16}$$

and calculate the frequencies of the first five mechanical modes (see Table 3).

Mode	Eigen Frequency
1	1405.04
2	1573.95
3	1609.63
4	1687.82
5	1712.62

Table 3. Eigen frequencies [Hz] of the first five modes for the problem (1-3) and the boundary conditions (12-14, 16).

Utilizing the harmonic response solver, we performed a frequency sweep from 1400 to 1750 Hz and identified the resonances by plotting the maximum amplitude of the displacements in all three directions (see Fig. 5).

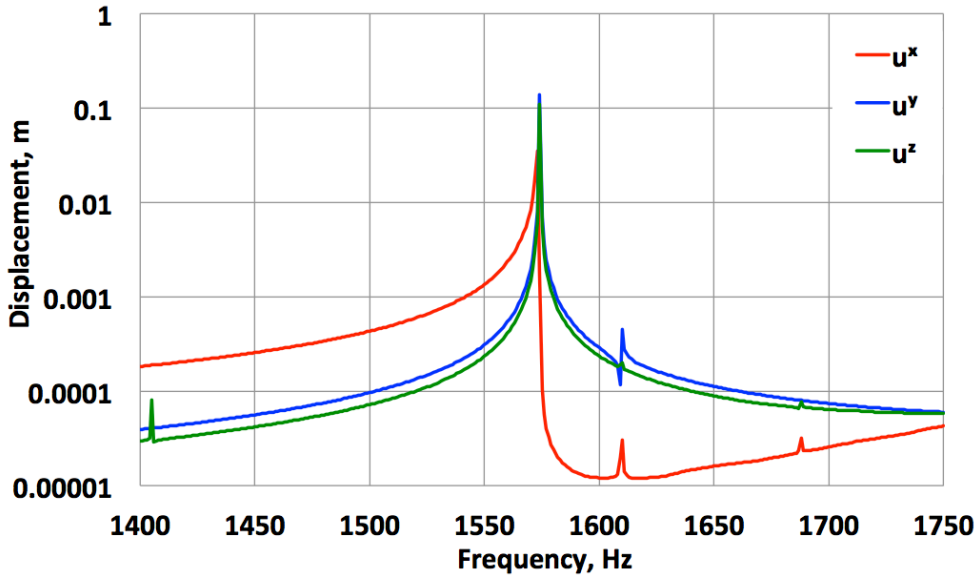

Figure 5. Maximum displacements for the frequency sweep using the harmonic response solver for the problem (1-3) and the boundary conditions (12-15).

As expected, the spikes (resonant frequencies) identified in Fig. 5 correspond to the eigen frequencies from Table 3.

5. Example of a Large-Scale Simulation

To illustrate the capability to handle realistic large-scale problems, we consider the TESLA superconducting accelerating cavity situated in a helium tank [16]. See Fig. 6 for details and Table 4 for the corresponding material properties. The contacts between different parts of the model are assumed to have no separation and no slip, i.e. bonded contacts, and, in building a corresponding mesh, tetrahedral elements do not cross the interface between the materials. To properly describe the cavity shape, curvilinear tetrahedral elements are employed.

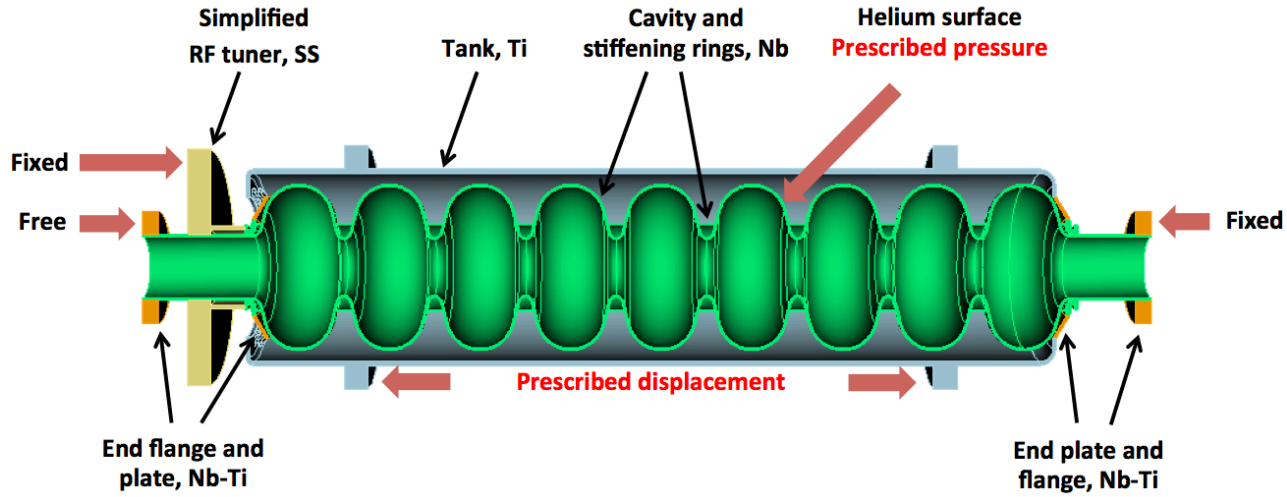

Figure 6. Superconducting TESLA cavity in a tank; the total structure length is 1.28 m

Property	Nb	Nb-Ti	Ti	SS
Density, ρ [kg/m^3]	8700	5700	4540	8000
Poisson Ratio, υ	0.38	0.33	0.37	0.29
Young's Modulus, E [GPa]	118	68	117	193

Table 4. Mechanical properties of the materials used in the simulation of the TESLA cavity.

The liquid helium is not included in the simulation and instead of a microwave tuner attached to the cavity wall, a simplified model with comparable stiffness is considered. We model a half of the radially symmetric structure and prevent any deformations perpendicular to the symmetry plane.

Simulation Parameter	Value
Number of Cores	240
Mesh Size	1.2 M
Number of Degrees of Freedom	5.7 M
Mesh Type	Curved Tetrahedrons
Number of Frequency Steps	201
Solver Time	1542 s

Table 5. The simulation profile for the harmonic response calculation in ACE3P.

The ACE3P simulation was performed on Edison, NERSC Cray XC30 supercomputer [17], see the simulation details in Table 5. A comprehensive eigenmode analysis was also performed for this model in [11] and the first five eigen frequencies (74 Hz, 74 Hz, 160 Hz, 160 Hz and 220 Hz) as well as the corresponding displacements, stresses and strains have been determined.

Here we consider two types of the harmonic excitations highlighted in red in Fig. 6: a) prescribed pressure on the He surface, i.e. inhomogeneous Neumann boundary condition (5) and b) prescribed displacement on the tank ring, i.e. inhomogeneous Dirichlet boundary condition (4).

We perform two independent simulations for these two types of the external excitations:

a) a frequency sweep from 50 to 250 Hz with a step of 1 Hz and the external surface pressure of 2.38e5 Pa [18], see Fig. 7. The spike observed at the frequency 220 Hz corresponds to the fifth eigenmode of the cavity determined in [11].

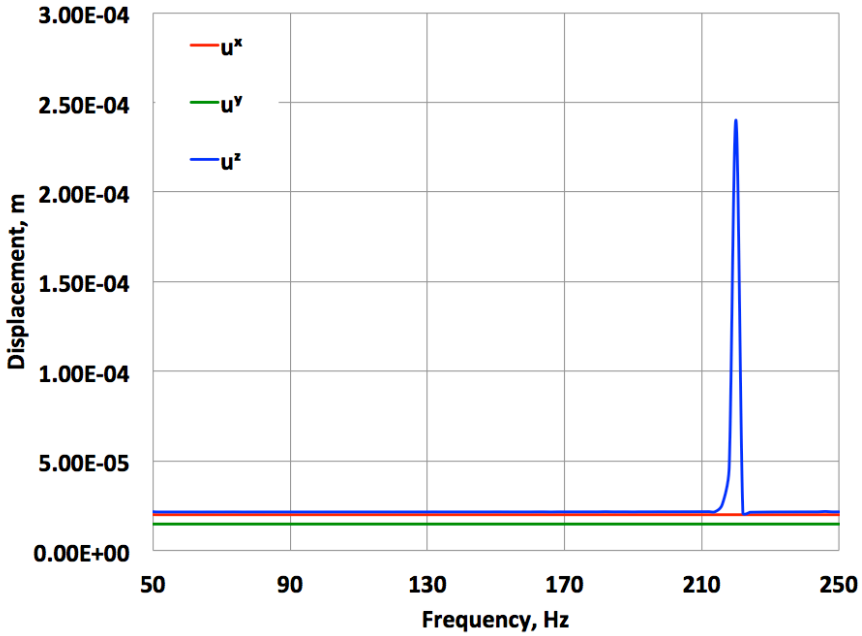

Figure 7. a) the maximum displacements for the frequency sweep using the ACE3P harmonic mechanical solver for the Tesla cavity in a cryostat, the external surface pressure is 2.38e5 Pa.

The corresponding displacement magnitudes are plotted at 74 Hz (the first eigenmode) and 220 Hz (the fifth eigenmode) in Fig. 8. One can see that the first eigen mode is off resonance and the excitation mostly absorbed by the bellows connecting the cavity to the tank, while the harmonic response of the system at 220 Hz is coupled to the fifth eigenmode identified in [11].

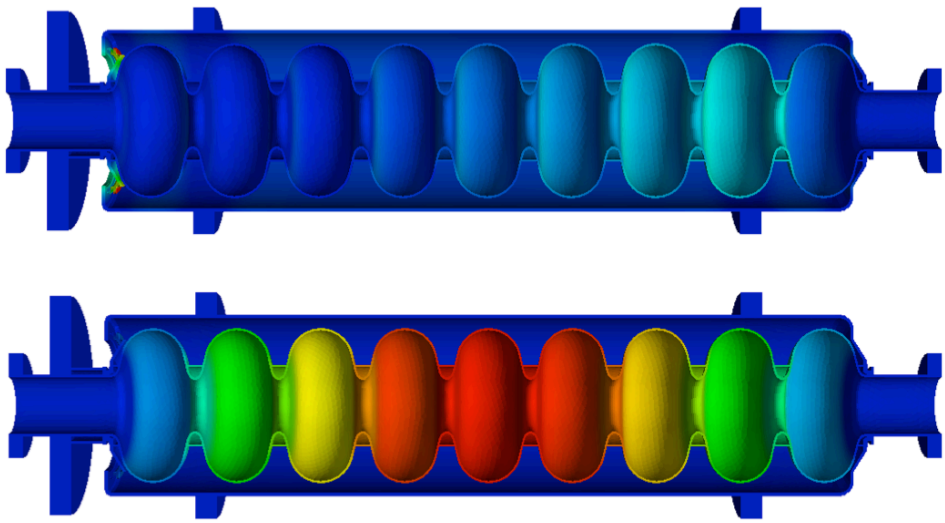

Figure 8. Displacement magnitudes at 74 Hz (top) and 220 Hz (bottom) plotted on top of the undeformed geometry for the He surface excitation, case a).

b) The same frequency sweep has been performed fixing the magnitude of the oscillation for the tank ring at the level of 1e-6 m, see Fig. 9.

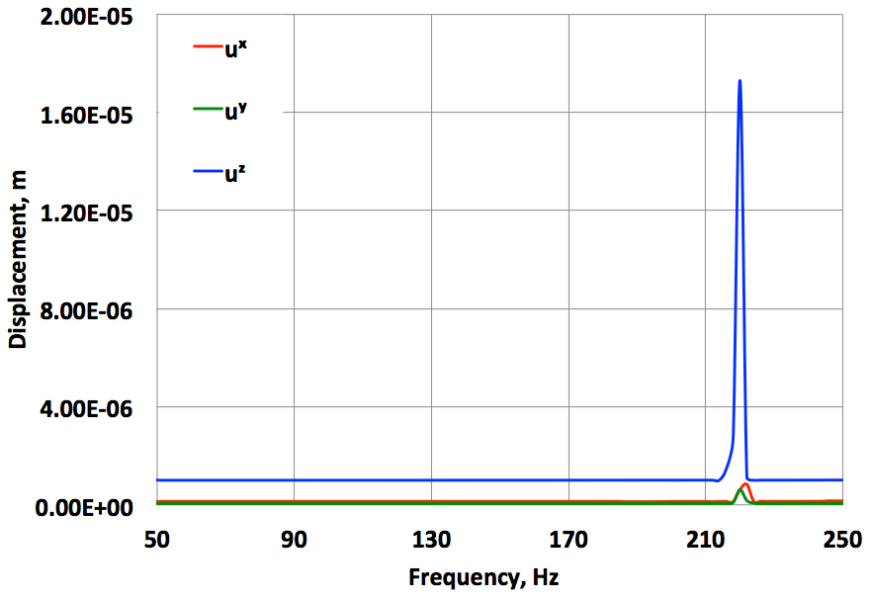

Figure 9. b) The maximum displacements of the Tesla cavity in a cryostat for the frequency sweep using the ACE3P harmonic mechanical solver, the magnitude of the oscillation for the tank ring is 1e-6 m.

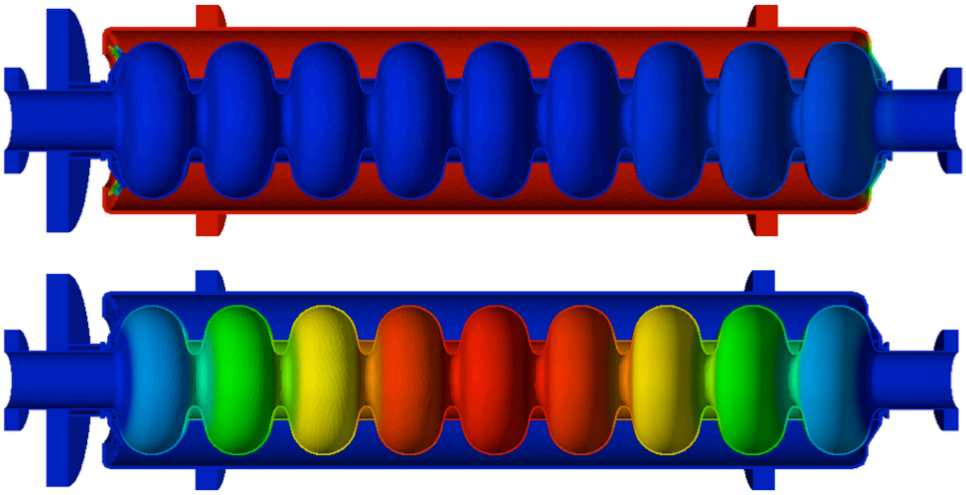

Figure 10. Displacement magnitudes at 74 Hz (top) and 220 Hz (bottom) plotted on top of the undeformed geometry for the ring excitation.

In Fig. 10 the displacement magnitudes are plotted at 74 Hz and 220 Hz. On the top picture one can see that the first eigen mode is not coupled to the external vibration and the response is mostly concentrated within the tank, while the harmonic response of the system at 220 Hz corresponds to the fifth eigenmode of the cavity [11].

In both cases the external harmonic loading couples to the longitudinal eigenmode of the cavity and a comprehensive analysis must be performed in order to understand the effect of the corresponding deformations on the operating RF frequency of the accelerating structure. It should be mentioned that the fluctuations in the He pressure [18] can be modeled using the

scheme discussed in case a) while the ground motion or other types of the environment vibrations can be studied in a way similar to b).

The main advantage of the developed ACE3P harmonic response solver, i.e. the capability to perform a time-efficient accurate harmonic analysis of the complicated mechanical structures utilizing supercomputer resources, has been demonstrated. The solution for a problem with millions degrees of freedom can be processed in seconds.

As discussed in Section 3, the harmonic response solver uses the linear solvers implemented in ACE3P, requiring the solution of a linear system at each frequency step using a direct or an iterative solver. In Fig. 11 the strong scalability of the harmonic response solver using a direct linear solver on Edison, the Cray XC30 supercomputer at NERSC, is compared against the perfect linear scalability. It can be seen that for the simulation profile described in Table 5 it scales fairly well up to 400 processors.

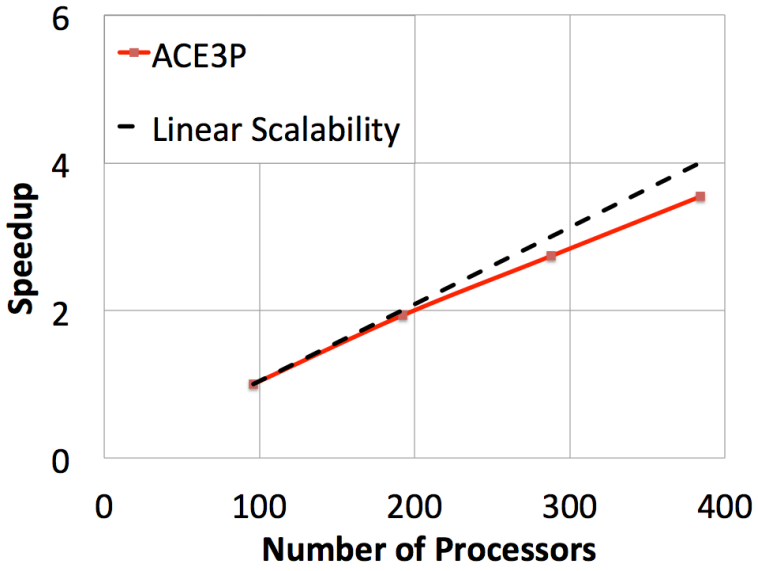

Figure 11. The strong scalability of the ACE3P mechanical eigensolver using direct linear solver (red) on Edison, the Cray XC30 supercomputer at NERSC, and the perfect linear scalability (black).

6. Conclusions

A mathematical model for harmonic response analysis in structural mechanics is derived based on the finite-elements method. A new massively parallel harmonic response solver is developed as a part of the ACE3P simulation suite. The proposed method has a quick convergence and the obtained results are in good agreement with those calculated in ACE3P eigenmodes solver and ANSYS.

One of the major advantages of ACE3P is that it can handle large-scale problems utilizing supercomputer resources and, as shown, can be used for a time-efficient harmonic response analysis of complicated mechanical structures. This new code capability is used in the multiphysics analysis of superconducting cavities for the LCLS-II project [19] involving the other ACE3P modules and helps understand the RF response and feedback requirements of accelerating structures to microphonics.

Acknowledgements

The work was supported by U.S. Department of Energy under Contract No. DE-AC02-76SF00515. This research used resources of the National Energy Research Scientific Computing Center, which is supported by the Office of Science of the U.S. DOE under Contract No. DE-AC02-05CH11231.

References

[1] Bishop, Richard Evelyn Donohue, and Daniel Cowan Johnson. The mechanics of vibration. Cambridge University Press, 2011.

[2] B. Aune, R. Bandelmann, D. Bloess, B. Bonin, A. Bosotti, M. Champion, C. Crawford et al. "Superconducting TESLA cavities", Physical Review Special Topics-Accelerators and Beams, Vol. 3, No. 9, 2000, 25 pages.

[3] I. Gonin, M. Awida, E. Borissov, M. Foley, C. Grimm, T. Khabiboulline, Y. Pischalnikov, V. Yakovlev, "Update of the mechanical design of the 650 MHz beta=0.9 cavities for project X", Proceedings of IPAC2013, Shanghai, China, 2013, pp. 2432-2434

[4] Ayvazyan, V T ; Simrock, Stefan, Dynamic Lorentz Force Detuning Studies in TESLA Cavities, 9th European Particle Accelerator Conference, Lucerne, Switzerland, 5 - 9 Jul 2004, pp.994

[5] O. C. Zienkiewicz, R. L. Taylor, The finite element method for solid and structural mechanics, Butterworth-heinemann, 2005, 736 pages.

[6] ACE3P Simulation Suite, SLAC National Accelerator Laboratory, http://www-group.slac.stanford.edu/acd/

[7] Kwok K, et al., Advances in parallel electromagnetic codes for accelerator science and development, Proceedings of Linear Accelerator Conference, Tsukuba, Japan, 2010, 5 pages

[8] K. Lee, et al., Multiphysics Applications of ACE3P, Proceedings of International Particle Accelerator Conference, Luisiana, USA, 2012, 3 pages

[9] L. Ge, K. Ko, K. Lee, Z. Li, C.-K, Ng, L. Xiao, Analyzing multipacting problems in accelerators using ACE3P on high performance computers, Proceedings of International Computational Accelerator Physics Conference, Rostock-Warnemünde, Germany, 2012, 5 pages

[10] W. S. Slaughter, The linearized theory of elasticity, Birkhauser, 2002, 543 pages.

[11] O. Kononenko et al., A Massively-Parallel Finite-Element Eigenvalue Solver for Modal Analysis in Structural Mechanics, SLAC Publication, SLAC-PUB-15976, 15 pages.

[12] Strauss, Walter A. "Partial differential equations: An introduction." New York, 1992, 454 pages.

[13] D.-K. Sun, J.-F. Lee, Z. Cendes, Construction of nearly orthogonal Nedelec bases for rapid convergence with multilevel preconditioned solvers, SIAM Journal on Scientific Computing, Vol. 23, No. 4, 2001, pp. 1053-1076.

[14] V. Akcelik, A. Candel, A. Kabel, L-Q. Lee, Z. Li, C-K. Ng, L. Xiao and K. Ko, Parallel computation of integrated electromagnetic, thermal and structural effects for accelerator cavities, SLAC-PUB-13280, SLAC National Accelerator Laboratory, 2008, 3 pages.

[15] ANSYS Workbench, Release 15.0

[16] B. Aune, R. Bandelmann, D. Bloess, B. Bonin, A. Bosotti, M. Champion, C. Crawford et al. "Superconducting TESLA cavities", Physical Review Special Topics-Accelerators and Beams, Vol. 3, No. 9, 2000, 25 pages.

[17] National Energy Research Scientific Computing Center, Office of Science and U.S. Department of Energy, http://www.nersc.gov/

[18] Wands, B., and M. Wong. "Pressure Vessel Engineering Note for the 1.3-GHz Helium Vessel, Dressed Cavity AES-004." (2013).

[19] Z. Li, L. Xiao, O. Kononenko, C. Adolphsen, M. Ross, T. Raubenheimer, “Multi-Physics Analysis of CW Superconducting Cavity For the LCLS-II Using ACE3P”, 5th International Particle Accelerator Conference, 2014, Dresden, Germany.